

Adsorbate Structure on Reconstructed Semiconductors: Te and I on Si{111}7×7 and Ge{111}2×8

P. H. Citrin, P. Eisenberger,^(a) and J. E. Rowe
Bell Laboratories, Murray Hill, New Jersey 07974

(Received 3 December 1981)

Studies of surface extended x-ray-absorption fine structure reveal unexpected adsorption site variations for I and Te adsorbed on Si and Ge surfaces. Iodine is found to occupy the atop site on both Si{111}7×7 and Ge{111}2×8 whereas Te occupies two distinct and previously unreported bridging sites on these surfaces.

PACS numbers: 68.20.+t, 78.70.Dm

The existing body of knowledge on adsorption site geometries on metals, where bonding is largely nondirectional, gives little guidance for predicting overlayer structures on semiconductors. The directional bonding of semiconductors suggests that a local orbital approach based on saturation of dangling bonds might be successful in predicting their surface adsorption behavior. Previous adsorbate studies on reconstructed semiconductors¹⁻⁶ have been unable to test this idea by reliably determining adsorption sites and bond lengths, either because the overlayer structures lacked sufficiently long-range order or because the methods themselves could not provide complete information. We report the determination of these short-range structural parameters for Te and I adsorbed on clean Si{111}7×7 and Ge{111}2×8 surfaces by means of surface extended x-ray-absorption fine structure (SEXAFS), a technique which has been shown capable of yielding precise information on these quantities even without long-range order present.⁷ We find that I occupies the same adsorption site on both substrates whereas Te occupies not only a different site than I but different sites on each substrate. These latter sites have not been previously observed on a {111} surface. Three cases are consistent with bond saturation arguments, while Te on Ge{111} is not. Measured near-neighbor distances, site coordination numbers, and second-neighbor distances (where observed) are all consistent with a locally unreconstructed substrate in the presence of the adsorbates.

A local orbital picture of both Si{111} and Ge{111} surfaces would describe the adsorption of monovalent I as saturating the dangling bond in the atop site 1, see Fig. 1. The size and divalency of Te would similarly suggest adsorption in the twofold bridging site 2 for both of these surfaces. However, this latter site has not been reported for an adsorbate on any {111} surface. Also, occupation of the more conventional three-

fold bridging site 3 is suggested by the threefold coordination of I and Te in the bulk analog compounds GeI₂ and SiTe₂, which have Ge-Ge or Si-Si distances that are only ~10% larger than those in the unreconstructed surfaces. Finally, the different anion coordinations between SiTe₂ vs GeTe and SiI₄ vs GeI₂ would suggest *different* adsorption behavior for Si{111} and Ge{111} surfaces. It is therefore clear that even within the simple framework of a local orbital picture, *a priori* arguments for a particular adsorption site on a semiconductor surface should be viewed as highly incautious.

The SEXAFS experiments were performed at the Stanford Synchrotron Radiation Laboratory with equipment previously described.⁷ Samples were cleaned with Ar⁺ bombardment and resistive annealing, directionally dosed with I₂ or Te vapors, and annealed at ~400 °C for 5 min with coverages of ~1 monolayer determined by Auger spectroscopy. Identical 7×7 low-energy electron-diffraction (LEED) patterns⁸ with weak seventh-order diffraction beams were observed for both I and Te overlayers on Si{111}7×7 (see inset, Fig. 2). On Ge{111}2×8, a simple 1×1 pattern was observed for I, while for Te the 1×1 pattern initially present changed to a 2×2 pattern upon annealing along with a reduction in coverage to

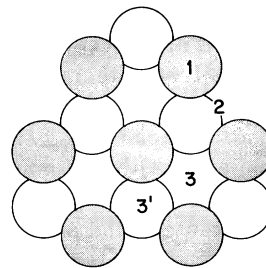


FIG. 1. First- (shaded) and second-layer atoms in unreconstructed Si, Ge{111} showing highest-symmetry adsorption sites.

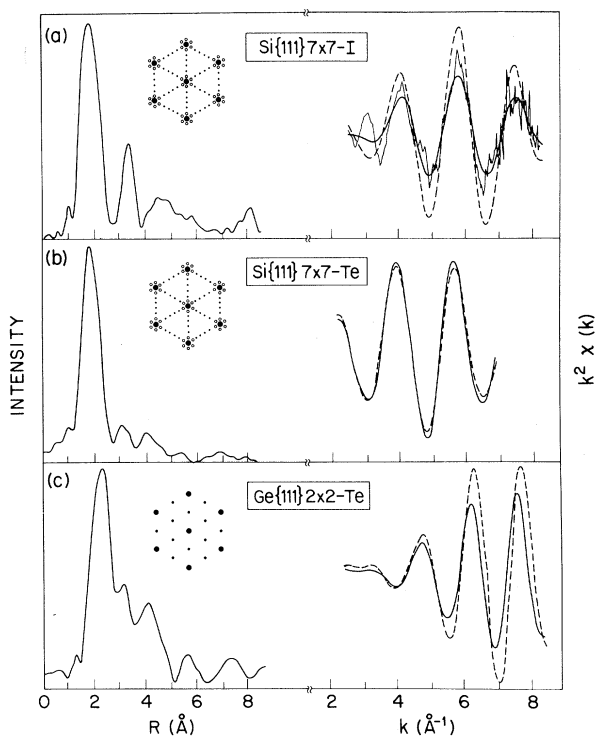


FIG. 2. Fourier-transformed SEXAFS data (left) taken at $\theta = 90^\circ$ with corresponding observed LEED patterns. Background-subtracted raw data at $\theta = 90^\circ$ are also shown in (a). Polarization-dependent filtered data of first nearest neighbors (right) taken at $\theta = 90^\circ$ (solid) and $\theta = 35^\circ$, 50° , and 35° (dashed) for (a), (b), and (c), respectively. Filter functions span 1.0–3.0 Å for (a) and (b) and 1.2–3.4 Å for (c). Note differences in amplitude and phase dependence with θ between (a), (b), and (c).

~ 0.5 monolayer. SEXAFS data from the I and Te L_{III} edges were taken in the total yield mode as a function of angle θ , measured between the synchrotron polarization direction $\vec{\epsilon}$ and the surface normal.

In Fig. 2(a) we show the raw background-subtracted SEXAFS data, its Fourier transform, and the back-transformed first-nearest-neighbor (nn) filtered data of Si{111}7 \times 7-I for $\theta = 90^\circ$.^{9,10} The filtered data are also compared with that taken at $\theta = 35^\circ$. The compound SiI(CH₃)₃, measured in transmission as a vapor, and its I-Si distance of 2.46 ± 0.02 Å (Ref. 11) are used to determine the first-nn I-Si{111} distance $R_1 = 2.44 \pm 0.03$ Å. The effective surface atom coordination numbers N_s (Ref. 7) for different θ values, determined with respect to $N = 1$ in SiI(CH₃)₃, are given in Table I and compared with those calculated^{7,12} on the assumption of occupation in the sites shown in Fig. 1. The calculated values for sites 2, 3, and 3' represent the sum of contributions from the atoms at R_1 and the second-nn substrate atoms at R_2 weighted by $(R_1/R_2)^2$.¹³ The absolute amplitude values immediately identify the atop position, 1. This is independently confirmed from the experimental relative SEXAFS amplitude (see Table I) which avoids reference to the model system.⁷ A third procedure is made possible by the observation of R_2 .¹⁰ Its value of 4.01 ± 0.04 Å in the $\theta = 90^\circ$ data is in close agreement with the calculated value of 3.91 ± 0.03 Å assuming site 1 on an unrelaxed Si{111}1 \times 1 substrate. The 0.1 Å larger value of R_2 suggests outward relaxation of the surface Si atoms.

A similar analysis of I adsorbed on Ge{111}2 \times 8 (yielding Ge{111}1 \times 1-I) with use of GeI₄ vapor¹⁴ gives results essentially indistinguishable from those of I on Si{111}7 \times 7, with $R_1 = 2.50 \pm 0.04$ Å and the adsorption site (see Table I) again being 1. The observed value of $R_2 = 4.06 \pm 0.05$ Å in the Ge{111}1 \times 1-I structure is very close to that calculated on the assumption of an unrelaxed Ge{111}1 \times 1 substrate, 4.04 Å. With the bond lengths and adsorption sites well established in these two systems if we assume locally unrecon-

TABLE I. Calculated vs experimental N_s values for I and Te on Si{111}7 \times 7 and Ge{111}2 \times 8.

	Calc.				Expt.			
	1	2	3	3'	I/Si	I/Ge	Te/Si	Te/Ge
$\vec{\epsilon}_{\parallel}^a$	0.7	2.7	5.3	3.0	0.7 ± 0.2	0.9 ± 0.2	3.0 ± 0.4	2.9 ± 0.4
$\vec{\epsilon}_{\perp}^b$	1.3	3.0	5.1	3.8	1.4 ± 0.3	1.8 ± 0.4	2.9 ± 0.4	4.0 ± 0.5
$\vec{\epsilon}_{\perp}/\vec{\epsilon}_{\parallel}^c$	1.9	1.1	1.0	1.3	2.0 ± 0.2	2.0 ± 0.3	1.0 ± 0.2	1.4 ± 0.2

^aCorresponds to $\theta = 90^\circ$.

^bCorresponds to $\theta = 35^\circ$, 40° , 50° , and 35° for I/Si, I/Ge, Te/Si, and Te/Ge, respectively.

^cThe relative amplitudes (i.e., the ratios) are determined without reference to the model compound, thereby explaining the smaller experimental uncertainties.

structed surfaces, we conclude that the short-range overlayer structures on initially complex clean reconstructed surfaces are relatively simple.

The Fourier-transformed and filtered SEXAFS data for Te adsorbed on Si{111}7×7 and Ge{111}2×8 [see Figs. 2(b) and 2(c)] clearly indicate that the adsorption sites are different for Te and I. In our structural analysis of adsorbed Te we have used SiI(CH₃)₃ and GeI₄. This approximation can be shown to provide (correctable) bond length errors of only ~0.01 Å and absolute amplitude errors of ≤10% (Ref. 15) (relative amplitudes are unaffected). Inspection of both relative and absolute SEXAFS amplitudes in Table I easily rules out sites 1 and 3 but the unambiguous distinction between sites 2 and 3' appears less straightforward and requires the use of amplitude and distance information. For Te on Si{111}7×7, R_2 is only ~0.1, ~0.4, and ~0.4 Å longer than R_1 for Te in sites 2, 3, and 3', respectively, and separate Fourier peaks cannot be resolved. This implies not only larger measured total amplitudes from atoms at R_1 and R_2 , i.e., $A = A(R_1) + (R_1/R_2)^2 A(R_2)$,¹⁶ but also larger measured average bond lengths, i.e., $\bar{R} = \alpha R_1 + (1 - \alpha) R_2$, $\alpha = A(R_1)/A$. The average Te-Si{111} distance $\bar{R} = 2.47 \pm 0.03$ Å therefore corresponds to first-neighbor distances of $R_1 = 2.44, 2.23,$ and 2.17 Å for Te in sites 2, 3, and 3', respectively. Comparing these values with the sum of tetrahedral covalent radii,¹⁷ 2.49 Å, and noting that LEED studies of chalcogens on a variety of substrates¹⁸ report R_1 values typically within ~0.1 Å of covalent radii sums, we conclude that only the twofold distance is physically reasonable. Our identification of site 2 on a {111} surface appears to be the first of its kind. It is understandable *a posteriori* that divalent Te would favor a twofold bridging site on Si{111} (one electron per dangling bond), especially in view of its size and the observed onefold adsorption behavior of monovalent I. Independent evidence for our assignment would be the observation of R_3 (R_4) distances at 3.65 (3.72) Å more strongly resolved than the structure seen in Fig. 2(b).

Data for Te adsorbed on Ge{111}2×8 [yielding Ge{111}2×2-Te, see Fig. 2(c)] show three features which are in sharp contrast with the other systems studied: (i) The main Fourier peak at about 2.3 Å (corresponding to ~2.7 Å including the phase shift) is significantly longer—by ~0.2 Å—than the sum of tetrahedral covalent radii,¹⁷ (ii) this distance is anisotropic, differing by 0.08

±0.02 Å for the two different θ values measured, and (iii) the relative and absolute SEXAFS amplitudes disagree with the conventional adsorption sites 1, 2, or 3 [see Fig. 2(c) and Table I]. We can explain these results by proposing that Te occupies site 3' in alternate rows on unreconstructed Ge{111}1×1.¹⁹ Such a site has also not been previously reported. Clearly the bonding picture here is more complex than that of the other Te and I structures studied, namely, adsorbates saturating dangling bonds on locally unreconstructed surfaces to achieve unity bond order. We note that our model does not explain either the higher-distance structure (>3 Å) observed in the Fourier-transformed data or why the annealed surface has the observed 2×2 LEED pattern. One possible explanation might be that unlike the other systems, deeper layers (1–4) of the Ge{111} substrate significantly distort upon adsorption and produce additional reconstruction of 2×2 periodicity due to adatom interactions. If this occurred, characterization of such long-range structure would be beyond the capabilities of our present analysis and further work would be needed to answer these questions.

In summary, we have determined both the bond length and the site geometry of adsorbates on initial Si{111}7×7 and Ge{111}2×8 surfaces assuming the adsorbate-covered surfaces to be locally unreconstructed. The overlayer structures exhibit short-range features which are rather straightforward, but the long-range properties suggest relaxation and/or reconstruction. The present work serves to demonstrate the simplicity of local chemisorbed overlayer structures on semiconductors (relative to clean substrates) as well as their complexity in terms of predictive chemical trends. We find that I occupies the same site on Si{111} and Ge{111}, but that Te behaves differently from I and differently for each substrate. Thus, of the four high-symmetry adsorption sites possible for these surfaces, three have been identified, two have not been previously reported, and none corresponds to the most common threefold site observed for {111} metal surfaces.

We are indebted to R. C. Hewitt for his skillful development of the sample interchange and annealing mechanisms. We also gratefully thank the entire Stanford Synchrotron Radiation Laboratory (SSRL) operations staff and directorate body for their generous assistance and support. The work done at SSRL was supported by the National Science Foundation through the Division of

Materials Research.

^(a)Present address: Exxon Research and Engineering, Linden, N. J. 07036.

¹R. Ludeke and A. Koma, *Phys. Rev. Lett.* **34**, 1170 (1975).

²P. Pianetta, I. Lindau, C. M. Garner, and W. E. Spicer, *Phys. Rev. Lett.* **35**, 1356 (1975).

³K. C. Pandey, T. Sakurai, and H. D. Hagstrum, *Phys. Rev. Lett.* **35**, 1728 (1975).

⁴J. A. Appelbaum and D. R. Hamann, *Phys. Rev. Lett.* **34**, 806 (1975).

⁵M. Schlüter, J. E. Rowe, G. Margaritondo, K. M. Ho, and M. L. Cohen, *Phys. Rev. Lett.* **37**, 1632 (1976).

⁶J. Stöhr, R. S. Bauer, J. C. McMenamin, L. I. Johansson, and S. Brennan, *J. Vac. Sci. Technol.* **16**, 1195 (1979).

⁷P. H. Citrin, P. Eisenberger, and R. C. Hewitt, *Phys. Rev. Lett.* **41**, 309 (1978), and **45**, 1948 (1980).

⁸These patterns have also been referred to as 1×1; see Ref. 5.

⁹For details of data analysis, see Ref. 7 and P. A. Lee, P. H. Citrin, P. Eisenberger, and B. M. Kincaid, *Rev. Mod. Phys.* **53**, 769 (1981).

¹⁰Differences between raw and first-*nn* filtered data in Fig. 2(a), particularly at low *k*, are due to additional SEXAFS from second-*nn* atoms (a filter from 2.4 to 4.4 Å is used for its analysis).

¹¹H. N. Rexroad, D. W. Howgate, R. C. Gunton, and J. F. Ollom, *J. Chem. Phys.* **24**, 625 (1956).

¹²Because the $(p \rightarrow s)(p \rightarrow d)$ cross term in the L_{III} -edge SEXAFS amplitude function is nonzero for anisotropic absorbers, N_S is modified from $\frac{3}{2} \sum_i (\frac{1}{3} + |\vec{\epsilon} \cdot \vec{r}_i|^2)$ (cf. Ref. 7) to $\frac{3}{2} \sum_i (1.4/3 + 0.6 |\vec{\epsilon} \cdot \vec{r}_i|^2)$ [cf. P. H. Citrin, P. Eisenberger, and R. C. Hewitt, *Phys. Rev. Lett.* **47**, 1567 (1981)]. The factor of $\frac{3}{2}$ is included here to account for appropriate normalization (cf. Lee *et al.*, Ref. 9).

¹³This weighting ignores differences between first- and second-*nn* atom Debye-Waller and inelastic loss terms, both of which could reduce the second-*nn* contribution.

¹⁴The I-Ge bond length in GeI₄ vapor is 2.50 ± 0.03 Å; M. W. Lister and L. E. Sutton, *Trans. Faraday Soc.* **37**, 393 (1941).

¹⁵This was verified theoretically from calculated values (cf. Lee *et al.*, Ref. 9) and empirically using Cu₂Te bulk EXAFS data.

¹⁶Although the second-*nn* atom amplitudes could contribute less than calculated here (see Ref. 13), it is unlikely that they would not contribute at all. For example, our adsorption site determination for Te/Si{111} would remain valid even if only 20% of our calculated contribution applied.

¹⁷L. Pauling, *The Nature of the Chemical Bond* (Cornell Univ. Press, New York, 1960), 3rd ed., p. 246.

¹⁸For example, see F. Jona, *J. Phys. C* **11**, 4271 (1978), and references therein.

¹⁹Assuming $R_1 = 2.45$ Å, we calculate average distances $R(35^\circ) = 2.74$ Å and $R(90^\circ) = 2.69$ Å, compared with observed values $R(35^\circ) = 2.74 \pm 0.04$ Å and $R(90^\circ) = 2.66 \pm 0.04$ Å.

Low-Frequency and Low-Temperature Raman Scattering in Silica Fibers

R. H. Stolen and M. A. Bösch

Bell Laboratories, Holmdel, New Jersey 07733

(Received 30 December 1981)

The Raman scattering spectrum of silica was measured to low temperature and very small frequency shifts. Strain-free cooling of a long silica-core fiber allowed us to investigate Raman scattering of the two-level tunneling systems to 1.5 K. A considerable central line broadening from relaxation of two-level tunneling systems is evident, although the predicted strong scattering contribution from resonant two-level tunneling centers at very low temperature and small frequency shift was not observed.

PACS numbers: 61.40.Df, 71.25.Mg, 78.30.-j

The Raman spectrum of silica at low temperatures and small frequency shifts is of particular interest because of the possibility of observing two-level tunneling systems which are characteristic of the amorphous state.¹⁻⁴ The two-level systems have been observed directly by ultrasonic absorption³ but their density of states can only be inferred from heat-capacity measurements.⁴ In this respect, a spectroscopic technique such

as far-infrared absorption or Raman scattering would be highly desirable. Two-level systems have been seen by far-infrared absorption between 2 and 12 cm⁻¹ in silica⁵ and silicate glasses.^{5,6} The relevant absorption is much stronger in the mixed glasses than in silica but, even there, difficulties with other absorption processes prevent the extraction of a reliable density of states.⁶ Relaxation processes associated with the two-